TU Delft

Delft University of Technology

Simulating the helix wake within an actuator disk framework verification against discrete-blade type simulations

Coquelet, M.; Moens, M.; Duponcheel, M.; Van Wingerden, J. W.; Bricteux, L.; Chatelain, P.

DOI
10.1088/1742-6596/2505/1/012017

Publication date
2023

Document Version
Final published version

Published in
Journal of Physics: Conference Series

Citation (APA)
Coquelet, M., Moens, M., Duponcheel, M., Van Wingerden, J. W., Bricteux, L., & Chatelain, P. (2023). Simulating the helix wake within an actuator disk framework: verification against discrete-blade type simulations. *Journal of Physics: Conference Series*, *2505*(1), Article 012017. https://doi.org/10.1088/1742-6596/2505/1/012017

Important note
To cite this publication, please use the final published version (if applicable).
Please check the document version above.

Copyright
Other than for strictly personal use, it is not permitted to download, forward or distribute the text or part of it, without the consent of the author(s) and/or copyright holder(s), unless the work is under an open content license such as Creative Commons.

Takedown policy
Please contact us and provide details if you believe this document breaches copyrights.
We will remove access to the work immediately and investigate your claim.

This work is downloaded from Delft University of Technology.
For technical reasons the number of authors shown on this cover page is limited to a maximum of 10.

Journal of Physics: Conference Series

PAPER • OPEN ACCESS

Simulating the helix wake within an actuator disk framework: verification against discrete-blade type simulations

To cite this article: M. Coquelet *et al* 2023 *J. Phys.: Conf. Ser.* **2505** 012017

View the article online for updates and enhancements.

You may also like

- (Invited) Thermodynamics, Stress, and Stefan-Maxwell Diffusion in Solids: Application to Small-Strain Materials Used in Commercial Lithium-Ion Batteries
Daniel R Baker, Mark W Verbrugge and Allan F Bower
- Special issue on applied neurodynamics: from neural dynamics to neural engineering
Hillel J Chiel and Peter J Thomas
- Information and Statistical Structure in Spike Trains
Jonathan D Victor and Emery N Brown

This content was downloaded from IP address 131.180.131.66 on 18/07/2023 at 14:25

Simulating the helix wake within an actuator disk framework: verification against discrete-blade type simulations

M. Coquelet[1,2], M. Moens[1], M. Duponcheel[1], J.W. van Wingerden[3], L. Bricteux[2], P. Chatelain[1]

[1] Université catholique de Louvain (Belgium), Institute of Mechanics, Materials and Civil Engineering
[2] Université de Mons (Belgium), Mechanical Engineering Department
[3] Delft University of Technology (The Netherlands), Delft Center for Systems and Control

E-mail: maud.moens@uclouvain.be

Abstract. Dynamic flow control strategies are raising interest for wake mitigation purposes. Among the different strategies, the so-called helix one relies on individual pitch control (IPC). The numerical simulation of the helix is thus readily performed by means of discrete-blade capturing methods. Yet, if this control strategy is considered at the scale of wind farms, the resolution required by such methods becomes prohibitive and actuator disk (AD) models should be envisioned. It is however not trivial to translate IPC strategies to an AD framework which by definition considers rotor-averaged effects. This work assesses the ability of an AD method to simulate the helix strategy by comparing it to a higher fidelity approach relying on a discrete-blade capturing model. Results show that the disk-type approach supplemented with a disk-adapted IPC scheme is able to capture both the forced motion of the wake at low turbulence and the faster wake recovery at moderate turbulence. From a quantitative perspective, the disk-type approach predicts bigger power gains, compared to those foreseen by the discrete-blade type approach, for a downstream turbine in the wake of a helix-operated one.

1. Introduction

Clustering wind turbines into wind farms creates an important challenge in terms of wake interaction. Many investigations have therefore emerged in the literature to mitigate wake effects and maximize wind farm power production [1]. More recently, dynamic flow control strategies have raised interest. One such strategy, called the helix and proposed by Frederik et al. [2], consists in using individual pitch control (IPC) in order to vary the fixed-frame tilt and yaw moments of the rotor over time. First numerical simulations have shown promising results regarding power production gains for a set of two aligned turbines.

In Frederik et al. [2], blades are modeled using the Actuator Line (AL) method. If one considers the numerical assessment of the helix control strategy at the scale of wind farms, the resolution required by the AL becomes prohibitive. The Actuator Disk (AD) model is an alternative as it relaxes resolution constraints. However, to the authors' knowledge, this control strategy has never been considered within an AD framework. This work aims at filling this gap in literature by investigating the ability of the AD method to simulate the helix strategy, with resolutions appropriate for wind farm simulations. To do so, we compare results obtained using a code in which the rotor is modeled with an AD method [3] to a higher fidelity approach relying on discrete-blade type modeling of the rotor [4, 5].

Content from this work may be used under the terms of the Creative Commons Attribution 3.0 licence. Any further distribution of this work must maintain attribution to the author(s) and the title of the work, journal citation and DOI.
Published under licence by IOP Publishing Ltd

The numerical tools and the control strategy are described in Section 2, while the numerical set-ups are presented in Section 3. Section 4 compares the loads and the wake of an isolated turbine operated with the helix control with the disk-type approach and the blade-type one. Section 5 quantifies the power gains to be expected in the case of a pair of in-line turbines. Finally, conclusions are drawn in Section 6.

2. Methodology

2.1. Numerical simulation tools

This work considers the Large Eddy Simulation (LES) of wind turbine wakes using two numerical solvers. The first one is adequate for wind farm simulations as it uses an actuator disk model and is thus well-suited for coarser spatio-temporal resolutions. The second one is as a higher fidelity method, used for verification, and relies on a discrete-blade type representation of the rotor. Note that both tools, which are described below, consider the rotor as a rigid body, i.e. the codes are not coupled to an aeroelastic solver for the structure. The tower and the nacelle are not represented in this work.

2.1.1. Fourth-order Finite Differences code with Actuator Disk method (FD4-AD)

We first consider a fourth-order finite differences code (FD4) solving the Navier-Stokes equations formulated in the velocity-pressure formulation and using a staggered mesh arrangement [6]. In the present study, the subgrid scale model is a Regularized Variational Multiscale variant [7] of the classical Smagorinsky model [8]. The inlet boundary condition is a uniform wind speed, over which turbulent fluctuations are imposed. Those are generated using the Mann algorithm [9]. A natural convective boundary condition is applied at the outflow and periodic boundary conditions are used in the lateral and vertical directions. The wind turbine is modeled using an AD approach and is added through external body force terms acting on the flow. The AD forces are distributed in the three directions using a second-order mollifier, the M_4 kernel [10]. The main equations and a description of the methodology can be found in Moens et al. [3].

As further described in Sec. 2.2, the helix strategy relies on individual pitch control (IPC), i.e. each blade imposes a different forcing on the flow. It is not trivial to translate such a strategy to a disk-type approach as it fundamentally considers rotor-averaged effects. Yet, the chosen AD model relies on non-uniform forces in radial and tangential directions. As demonstrated in Moens et al. [11], this allows for the AD to properly handle IPC strategies. The method also considers wake rotation effects and is supplemented with a tip-loss correction [3]. It is however not able to capture the individual tip vortices shed by the blades. At a phenomenological level, the helix strategy triggers vortical instabilities, which in turn destabilize the wake further downstream. This evidently raises the question of whether the AD approach can capture this disruption and motivates the present effort at verifying the AD predictions against a higher fidelity approach.

2.1.2. Vortex Particle-Mesh method with immersed Lifting Lines (VPM-LL)

The reference computations are performed using a Vortex Particle-Mesh (VPM) method [4]. It relies on the Lagrangian discretization of the Navier-Stokes equations in vorticity-velocity formulation. Advection is handled by particles. This ensures little numerical dispersion and dissipation and thus provides high accuracy when simulating turbulent flows and wakes. A mesh allows the evaluation of the differential operators and the use of a fast Poisson solver. The inlet boundary condition is a uniform wind speed, over which Mann-generated turbulent fluctuations can also be imposed. Unbounded conditions are enabled in the transverse directions [4].

The wind turbine is represented by a discrete-blade type approach consistent with the vorticity-velocity formulation, i.e. Lifting Lines (LL). Blades are seen as sources of vorticity that shed vortex particles in the wake. This makes the formulation compatible with the Lagrangian

formulation of the flow solver. Doing so preserves the efficiency and stability of the VPM method. This, combined to fine spatial resolutions, allows to accurately capture the tip vortices and their destabilization, hence we consider the VPM-LL [12, 13] approach as a reference.

2.2. The helix control

The helix control is a dynamic wake mitigation strategy as it forces sine-like variations of the tilting and yawing moments on the rotor. In low-turbulence conditions, this leads to substantial vertical and horizontal motions of the wake and, from there, its signature helical shape.

The variations of tilt and yaw moments at the rotor result from an individual pitch control, which is most known in the literature for load alleviation control [14]. As is commonly done for load-alleviating IPC [14], the helix control relies on the Coleman transform to correlate tilt and yaw rotor-associated quantities to blade-associated ones [15, 2]. More specifically, the blade pitch angles for the three blades, defined as β_1, β_2 and β_3, are recovered from tilt and yaw pitch setpoints, β_t and β_y respectively, following

$$\begin{pmatrix} \beta_1(t) \\ \beta_2(t) \\ \beta_3(t) \end{pmatrix} = \begin{pmatrix} \cos(\theta_1(t)) & \sin(\theta_1(t)) \\ \cos(\theta_2(t)) & \sin(\theta_2(t)) \\ \cos(\theta_3(t)) & \sin(\theta_3(t)) \end{pmatrix} \begin{pmatrix} \beta_t(t) \\ \beta_y(t) \end{pmatrix} \tag{1}$$

with θ_1, θ_2 and θ_3 the azimuthal position of the blades. For the discrete-blade type approach (VPM-LL), it is trivial to apply the individual blade pitch actions. For the disk approach (FD4-AD), in order to project $\beta_t(t)$ and $\beta_y(t)$ on the disk elements, we use the Coleman transform generalized for the n azimuthal elements of the AD

$$\begin{pmatrix} \beta_1(t) \\ \vdots \\ \beta_n(t) \end{pmatrix} = \begin{pmatrix} \cos(\theta_{AD,1}) & \sin(\theta_{AD,1}) \\ \vdots & \vdots \\ \cos(\theta_{AD,n}) & \sin(\theta_{AD,n}) \end{pmatrix} \begin{pmatrix} \beta_t(t) \\ \beta_y(t) \end{pmatrix} \tag{2}$$

with $\theta_{AD,1}, \ldots, \theta_{AD,n}$, the azimuthal position of the AD elements, and $\beta_1, \ldots, \beta_n$, the individual pitch angles. We highlight that this generalized Coleman transform was used in Moens et al. [11] for investigating load-alleviating IPC within the FD4-AD framework.

IPC is here used for wake mitigation purposes and the helix is implemented by imposing quadrature-phase sine setpoints for tilt and yaw pitch angles, with two possible options:

$$\beta_{\mathrm{t}}(t) = A\sin(2\pi f_{helix}\, t) \qquad \text{and} \qquad \beta_{\mathrm{y}}(t) = A\cos(2\pi f_{helix}\, t) \tag{3}$$

$$\beta_{\mathrm{t}}(t) = A\sin(2\pi f_{helix}\, t) \qquad \text{and} \qquad \beta_{\mathrm{y}}(t) = -A\cos(2\pi f_{helix}\, t)\,. \tag{4}$$

Assuming clockwise rotation of the turbine looking from upstream, the first actuation will result in a counterclockwise rotation of the wake helix (CCW), while the second corresponds to a clockwise rotation of the wake helix (CW). The parameters of the harmonic oscillations for the helix control are chosen to be similar to those defined in Frederik et al. [2]: an amplitude $A = 2.5^{\mathrm{o}}$ and a Strouhal number $St = f_{helix}D/U_{ref} = 0.25$, i.e. an actuation period $T_{helix} = 4\,D/U_{ref}$, where D is the wind turbine diameter and U_{ref} is the mean wind speed.

3. Numerical set-ups

Wake mitigation is particularly needed when turbines operate in under-rated wind speeds. Here we consider $U_{ref} = 9\,\mathrm{m/s}$ as this wind speed is representative of such conditions for the NREL 5MW [16], which is the simulated turbine in this paper. First, we perform simulations of a single wind turbine. This aims at assessing the FD4-AD approach when it comes to simulating

the helix at a coarse resolution by verifying it against the VPM-LL approach at a finer resolution. Second, we consider a configuration with two aligned wind turbines, separated by a $5D$-spacing, in order to highlight the influence of the helix control on the production of a downstream machine. The domain size, the resolution and the location of the wind turbine in each code are reported in Table 1. As in several AD methodologies, our disk approach implies exchanging information between the rotor mesh, which is polar, and the FD4 mesh, which is cartesian (details can be found in Moens et al. [3]). The radial and azimuthal resolutions of the polar mesh are fixed such that the largest polar cells are roughly the size of a cartesian cell. In this work, the disk thus has 10 elements in the radial direction, and 62 elements in the azimuthal direction (denoted "n" in Section 2.2).
Note that all the meshes used in the present work are uniform and do not involve local refinement in the rotor region or in its wake. Also, x, y and z represent the streamwise, vertical and spanwise directions, respectively. As the VPM method handles exactly the unbounded transverse directions y and z, the computational mesh can be taken tight around the physics of interest. The simulation domain for the FD4-AD approach is larger to limit the effect of boundaries on the wind turbine operation and the resulting wake behavior.

	Single turbine $TI = 1\%$ and $TI = 7\%$		Pair of turbines $TI = 7\%$	
	FD4-AD	VPM-LL	FD4-AD	VPM-LL
x-lim	$[-3D, 11D]$	$[-2D, 10D]$	$[-3D, 13D]$	$[-2D, 10D]$
y-lim, z-lim	$[-6D, 6D]$	$[-2D, 2D]$	$[-6D, 6D]$	$[-2D, 2D]$
D/h	16	64	16	64

Table 1: Domain extent in the three directions (x-lim, y-lim, z-lim), resolution (D/h, with $D = 126\,\mathrm{m}$ the diameter of the NREL 5MW and h the size of the mesh cell) for the disk-type approach (FD4-AD) and the blade-type one (VPM-LL). First turbine coordinates are $(0, 0, 0)$, while second turbine coordinates are $(5D, 0, 0)$.

In the single-turbine configuration, the wind turbine operates in a uniform flow with a very low turbulence level $TI = 1\%$ and with a more realistic level $TI = 7\%$. These two levels of turbulence will enable to discriminate between the effects of the controller and those of ambient turbulence. Note that we do not opt for an absolutely laminar flow but rather a TI of 1%. This helps to limit numerical effects regarding the triggering of the wake destabilization. In the two-turbine configuration, only the configuration with $TI = 7\%$ is studied.
In both codes, the turbulence field is generated using the Mann algorithm [9] and is added to the mean inflow velocity. In order to have a fair comparison between the two approaches, it is important that the same turbulent structures impact the wind turbine in the two codes. The same synthetic turbulence boxes for the FD4-AD and the VPM-LL methods are thus generated. Two boxes are generated: one with $TI = 1\%$ and the other with $TI = 7\%$.
The size of the turbulence boxes is set to $16D \times 4D \times 4D$. The initial resolution of the boxes generated with the Mann algorithm is $512 \times 128 \times 128$. As the FD4-AD and VPM-LL meshes have different resolutions ($D/h = 16$ and $D/h = 64$, respectively), the resolution of the turbulence field is adapted according to the method. As the initial turbulence box is smaller in terms of span than the FD4-AD simulation domain, the turbulent field is only added on a square of $4D \times 4D$ at the inflow, centered around the turbine position.
For all configurations, we consider the two helix control strategies described in Section 2.2 (CCW and CW). The actuation period is $T_{helix} = 4\,D/U_{ref} = 56\,\mathrm{s}$ in this context. Statistics are computed over the Mann box period, which covers 4 periods of actuation. Results are compared

against those, further referred to as STD, of a turbine operated with a standard variable-speed variable-pitch controller [16]. Note that this standard controller is also running as a background controller when the helix strategy is active.

In terms of computational cost, simulations performed with the FD4-AD approach required around 40 CPUh each, while those with the VPM-LL approach ran for 8000 CPUh each.

4. Single wind turbine

In this section, we assess the FD4-AD approach at the coarse resolution by comparing its predictions of the helical wake to those of the VPM-LL method with finer resolution.

4.1. Wind turbine behavior

We first compare the rotor loads for the two methods in Fig. 1, this is required to perform a fair analysis of the wake behavior as one needs to exclude potential discrepancies in the wake statistics resulting from differences in the rotor behavior. Whatever the control strategy and turbulence intensity, the predicted aerodynamic power is slightly higher for the FD4-AD method than for VPM-LL (+0.6% and +1.8%, on average for the STD case at $TI = 1\%$ and 7% respectively). The same remark holds for the thrust force (+1.2% and +2.2% on average for the STD case at $TI = 1\%$ and 7%, respectively). This slight overestimation of forces by the FD4-AD method was already reported in Moens et al. [3] and likely results from the coarse resolution of the disk. Indeed, the tip losses cannot be captured as accurately as with the higher line resolution. However, both methods capture a similar reduction of power production when the helix strategies are active, whether CCW or CW, as it will be further discussed in Section 5. The small reduction of the power production obtained for the turbulent inflow when the helix control is active was also observed in Frederik *et al.* [2]. In this research paper, the authors numerically investigated the behavior of the DTU-10 MW in wind conditions and wind turbine operation similar to those considered in this work, but using the SOWFA code and the AL method for the rotor representation. They also accounted for a more realistic representation of the wind environment, through the simulation of an Atmospheric Boundary Layer (ABL).

As the helix control consists in forcing a rotating moment on the rotor, Fig. 1 also presents the tilting (M_t) and yawing (M_y) moments resulting from the actuation. These show that the AD model supplemented by IPC as described in Sec. 2.2 is able to reproduce the same forcing as the one generated with a discrete-blade type approach. The amplitude of oscillation of the moments are indeed very similar with both numerical methods. Again, the periodic variations of M_t and M_y are similar to those observed in the numerical investigation of Frederik *et al.* [2].
A last comment on the loads concerns the signals computed with the VPM-LL method. These exhibit oscillations at high frequency, namely at a three-time per revolution frequency (3P). This is a direct translation of the discrete-blade type representation: harmonics on the 1P frequency appear on the blade loads, the 3P one results in 3P oscillations on all rotor quantities.

4.2. Wake behavior

After showing their good agreement in terms of loads computations, we now compare the FD4-AD and VPM-LL methods regarding wake topology, which is presented in Fig. 2.
A general comment is that wakes seem to be more recovered from $x/D = 4$ for the FD4-AD approach, whatever the control strategy. This is further discussed in Section 4.3.
We now discuss the effect of the helix control on the wake topology and begin with the $TI = 1\%$ simulations. The variations of yawing and tilting moments at the rotor leave a signature on the wake, with areas of stronger and weaker velocity deficits in the very near wake ($x/D = 0$ to 1). This is observable in Fig. 2(a), where the velocity deficit is stronger in the upper part of the

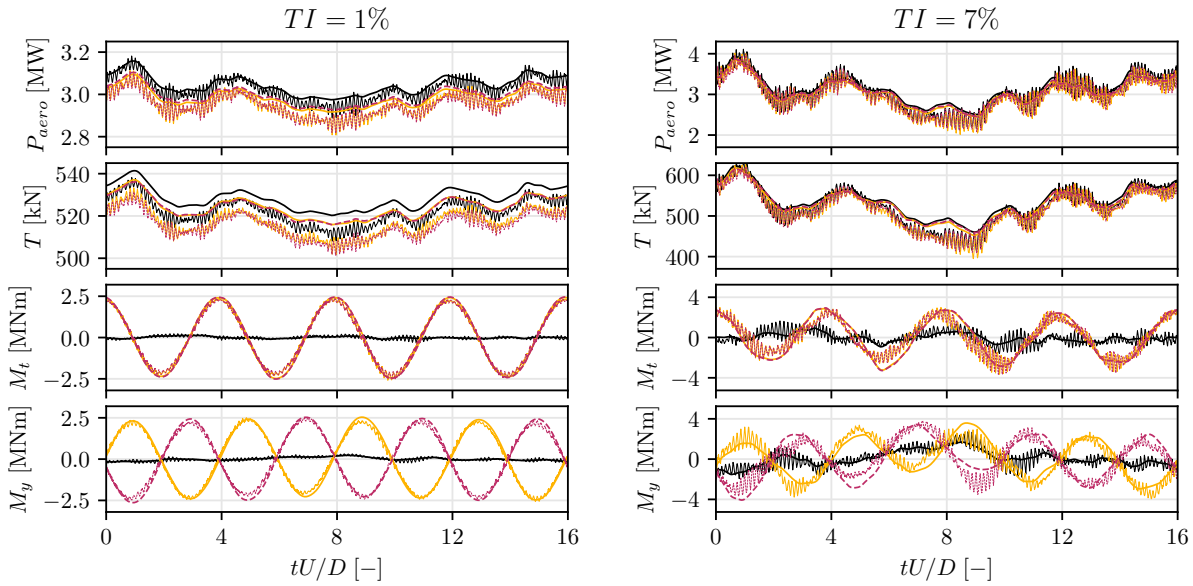

Figure 1: Aerodynamic power P_{aero}, thrust T, tilting moment M_t and yawing moment M_y under three operations: STD (——), CCW (——), CW (- - - - -). Results are provided for the two numerical methods: FD4-AD (thick line), VPM-LL (thin line); and for the two considered turbulent intensities: 1% (left), 7% (right).

slice than in its lower part for the CCW helix and conversely for the CW one. The same near wake behavior is observed with the VPM-LL approach in Fig. 2(b). When it comes to the far wake, the helix strategy is expected to generate large scale displacements of the wake, in the fashion of wake meandering, following the rotating forcing imposed at the rotor. In the CCW case, both numerical methods capture this forcing and similar large scale motions of the wake are captured. In the specific case of the CW helix, large displacements of the wake are also retrieved with the FD4-AD method, though they are not seen with the VPM-LL method.

When turbulence is higher ($TI = 7\%$), the zones of stronger/weaker wake deficit are still slightly observable in the very near wake, while the large scale motion of the far wake is not as observable. The presence of turbulence already induces wake meandering (see Fig. 2(a,b) (STD)), such that the patterns imposed by the helix blend into those resulting from the ambient turbulence. With the FD4-AD method, the wake seems more diffused with both the CCW and CW helix strategies. It is not as straightforward to extract a similar trend with the VPM-LL method. This will be further analyzed in the next section, with the computation of the available power in the wake.

4.3. Wake recovery and power gains in the wake

This section aims at quantifying the effects of the helix strategy on the wake deficit. To do so, we define $P_w(x,t) = \frac{1}{2}\rho\langle u_x^3(x,t)\rangle_w A$ as the power of the wind passing through a disk located behind the rotor, with $\langle u_x^3(x,t)\rangle_w$ the mean cubic streamwise velocity over the disk surface. That value is then time-averaged over 4 helix periods to provide $P_w(x)$, i.e. the power that would be available for a downstream turbine. The wake power is normalized using $P_0 = \frac{1}{2}\rho U_{ref}^3 A$.

This indicator, characterizing the wake recovery, is presented in Fig. 3. We first comment on the differences, in the STD case, between the two methods. In the near wake, the wake recovers faster with the VPM-LL method compared to the FD4-AD one. The effect is more marked at

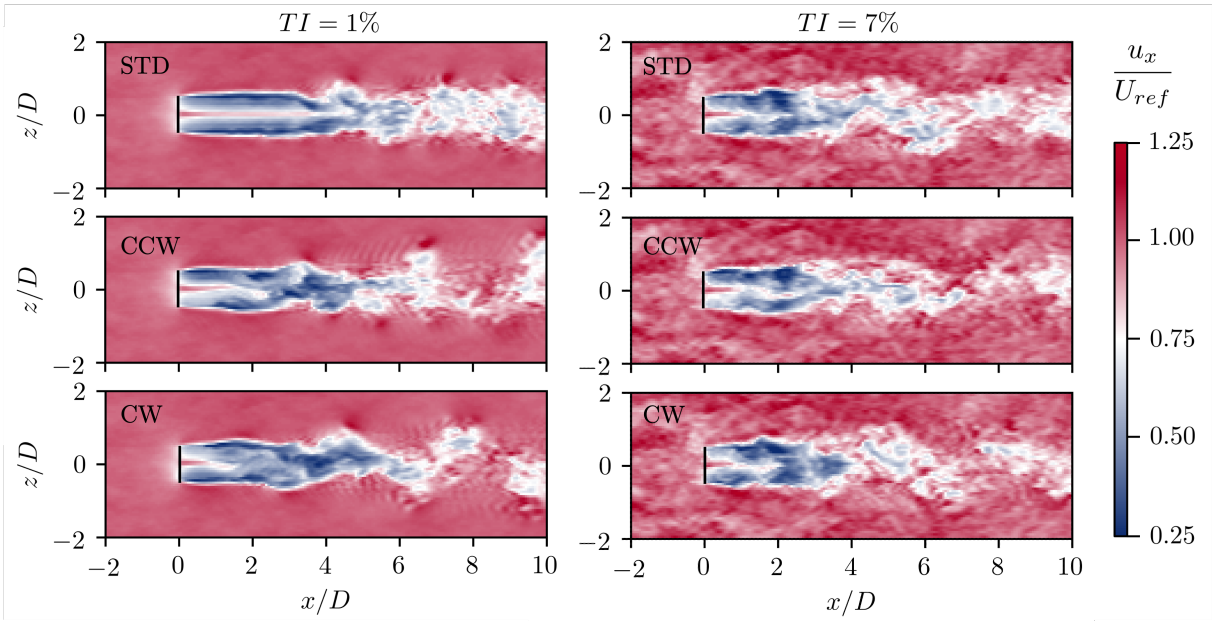

(a) FD4-AD

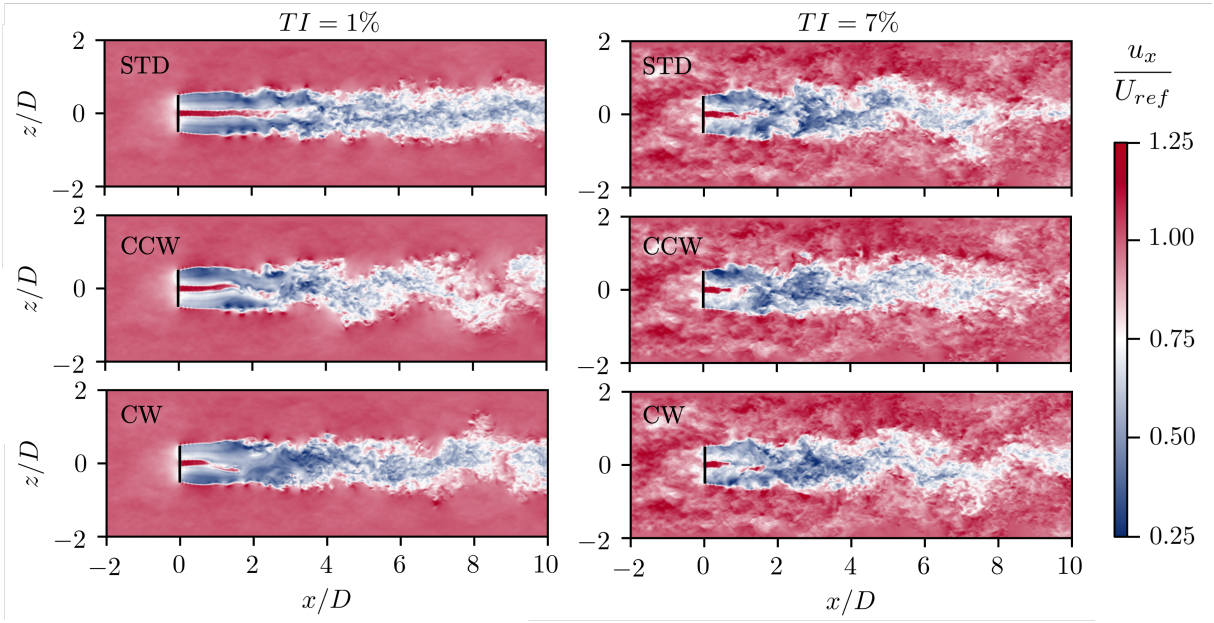

(b) VPM-LL

Figure 2: Instantaneous slice of streamwise velocity u_x under three operations: STD, CCW and CW. Results are provided for the two numerical methods (FD4-AD (a), VPM-LL (b)) and for the two considered turbulent intensities (1% (left), 7% (right)).

$TI = 1\%$, though it is also present at $TI = 7\%$. This is explained by the difference of resolutions between the two methods and their representation of the rotor. The wake destabilization starts when the shear layer at the edge of the wake, resulting from the difference of streamwise velocity inside and outside the wake, becomes unstable. With the FD4-AD method at coarse resolution, the shear layer is continuous and quite diffuse and thus takes longer to destabilize

(first oscillations around $x/D = 3$). Conversely, the shear layer of the VPM-LL method is sharper and marked by the shedding of discrete blade tip vortices, hence it destabilizes faster (first oscillations around $x/D = 1$). Discrepancies in the far wake are attributed to the wake topology. The FD4-AD wake destabilizes through large flow structure, while the VPM-LL one leads to the generation of smaller ones.

The relative increase in power available in the wake for the helix is then computed with respect to the standard control case following $\Delta P_w(x) = \frac{P_w(x) - P_w(x)^{\mathrm{STD}}}{P_w(x)^{\mathrm{STD}}}$. The power gains are computed for each code. When $TI = 1\%$, the FD4-AD method always predicts higher gains in the turbine wake than the VPM-LL method for the CW helix. For the CCW one, gains are higher with the FD4-method in the near wake but the trend is inverted from $x/D = 7$. Whatever the numerical method, gains are reduced when TI is taken to 7%. Indeed, the wake recovery is naturally enhanced by ambient turbulence, as confirmed by the $P_w(x)$ profiles. At such a turbulence intensity, the FD4-AD method estimates higher power gains resulting from the CCW and CW helices than the VPM-LL method. Indeed, it predicts power gains of 13% at $x/D = 5$ with the CCW helix, while only a 6% gain could be expected according to the VPM-LL method. More questionably, the FD4-AD considers a similar power gain behind the CW helix, while the VPM-LL method sees a slower wake recovery, i.e. a reduced power available in the wake.

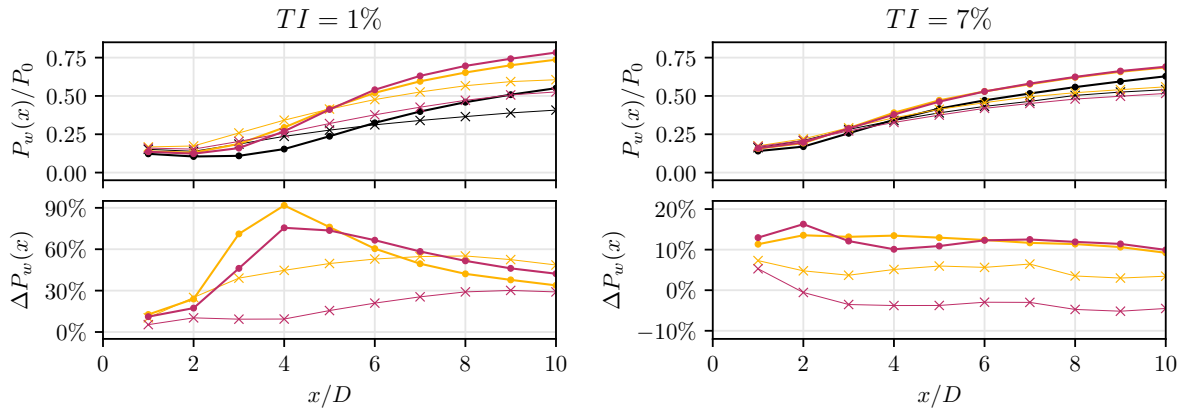

Figure 3: Power $P_w(x)$ available in the wake (top) under three operations: STD (——), CCW (——), CW (——). Power gain $\Delta P_w(x)$ with respect to STD (bottom) when using CCW (yellow line ——) or CW (purple line ——). Results are provided for the two numerical methods: FD4-AD (thick line with dots), VPM-LL (thin line with crosses); and for the two considered turbulent intensities: 1% (left), 7% (right).

5. Pair of in-line wind turbines

The first result section presented simulations of a single turbine and aimed at assessing the ability of the FD4-AD approach to simulate the helix strategy and its effects on the wake. This second result section presents simulations of a pair of in-line turbines and shows the overall power gains to be expected in such a configuration.

5.1. Power gains at the pair scale

Table 2 gathers the power production of the turbines as computed by the two solvers with the different controllers. While the power loss on the first turbine (WT1) when the helix control is active is captured by both numerical methods, the power increase on the second turbine (WT2)

is higher with the FD4-AD method, especially in the CW case. This is coherent with the wind power gains available in the wake presented in Fig. 3. At the pair scale when using the CCW helix, the power is expected to increase by 2.3% with the FD4-AD method, while only by 1.6% with the VPM-LL one. For the CW helix however, the FD4-AD method leads to a power gain of +2.1%, while the VPM-LL method captures a power loss of 3.6%. We note that, similarly to our FD4-AD results, Frederik *et al.* [2] obtained an increase of power on the second rotor in a line, both for CCW and CW helices. However, the total power gains are quite different from those obtained in the present study, with a more marked difference between the helix control cases: +3.4% for CCW helix and +0.8% for CW helix (see [2]).The wind conditions and wind farm environment (TI = 5%, realistic ABL representation, ground effect) are quite too different from those considered in our simulations to have a rigorous discussion about the discrepancies observed in the power gains.
The differences observed between FD4-AD and VPM-LL in terms of WT1 wake recovery (see Section 4.3) and the resulting WT2 power production for CW helix are quite intriguing and further investigations are needed. In a future work, we envisage to run simulations with several turbulence boxes (characterized by the same TI) and accumulate the power histories over those simulations. This will allow us to compute more consistent power statistics and could mitigate (or confirm) the differences observed in terms of WT2 power production between FD4-AD and VPM-LL. We also plan to run simulations using FD4-AD at a resolution similar to that used in VPM-LL in order to isolate the discrepancies related to the wind turbine representation from those related to the resolution.

	P_{WT1}		P_{WT2}		P_{TOT}	
	FD4-AD	VPM-LL	FD4-AD	VPM-LL	FD4-AD	VPM-LL
STD	3.13 MW	3.04 MW	1.25 MW	1.13 MW	4.39 MW	4.17 MW
CCW	3.05 MW	2.96 MW	1.43 MW	1.28 MW	4.49 MW	4.24 MW
	−2.5%	−2.5%	+14.2%	+12.7%	+2.3%	+1.6%
CW	3.07 MW	2.97 MW	1.40 MW	1.06 MW	4.48 MW	4.02 MW
	−1.8%	−2.4%	+11.8%	−6.8%	+2.1%	−3.6%

Table 2: Aerodynamic power of the two turbines for $TI = 7\%$ under three operations of WT1: STD, CCW and CW. Power gains with respect to STD when using CCW or CW.

5.2. Wake recovery and power gains in the wake
Finally, we analyze the wake recovery of the second turbine. Figure 4 shows the difference in time-averaged streamwise velocity in a horizontal plane when the helix control is active compared to the STD case. Results using the VPM-LL method show that the velocity is higher in the wake of WT2 when the CCW helix strategy is active on WT1. The trend is not as marked with the FD4-AD method, but this is worth of further investigations in the perspective of longer lines of turbines.
The length of the domain in the streamwise direction is quite small, and does not allow us to investigate wake statistics on long distances downstream of WT2. We plan to run simulations with larger domain in order to rigorously investigate the effect of the helix control on the WT2 wake behavior.

6. Conclusions and perspectives
The main part of this paper is dedicated to a thorough verification of a disk-type method at coarse resolution (FD4-AD) when it comes to the simulation of the helix control strategy. The

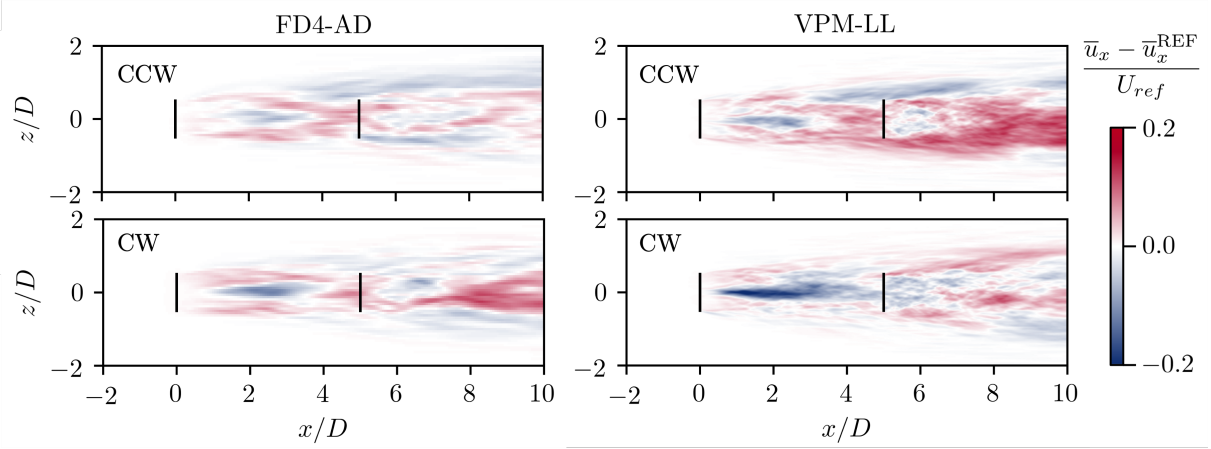

Figure 4: Slice of relative change in time-averaged streamwise velocity u_x for $TI = 7\%$ with CCW and CW with respect to STD. Results are provided for the two numerical methods.

assessment of the method is performed, both in terms of turbine loads and wake topology for one machine, by comparing results with a discrete-blade type approach at finer resolution (VPM-LL). We consider the latter as our reference as it produces a higher-fidelity reproduction of the rotor aerodynamics and wake physics.

Results show that, at very low turbulence, the helix control strategy forces a regular wake meandering, and thence the helical shape of the wake. Following the VPM-LL method, the forced wake meandering is more marked for the CCW helix than for the CW one. The AD approach cannot reproduce this difference in wake behavior between CCW and CW helix control schemes. At moderate turbulence, meandering is already present due to ambient turbulence and the helix strategy rather enhances wake destabilization. Another discrepancy between the two methods concerns the power production gains when the helix control is active. For the CCW helix, both methods predict power gains: +2.3% with FD4-AD, but only +1.6 with VPM-LL. However, the FD4-AD method foresees power gains (+2.1%) for a pair of in-line turbines for which the upstream turbine uses the CW helix, which was not observed with the higher-fidelity VPM-LL method (−3.6%).

As a global conclusion, this first study shows that the present disk-type approach, supplemented with a disk-adapted IPC scheme, is able to capture both the forced motion of the wake at $TI = 1\%$ and the faster wake recovery at $TI = 7\%$ of the CCW helix. This is encouraging as it opens the door for the evaluation of the helix strategy at the scale of large wind farms using Large-Eddy Simulations. A direct perspective is thus the simulation of longer lines of wind turbines. This would, among others, confirm whether turbines deeper in the line could also benefit from the helix actuation on the first turbine. However, the present AD framework deserves further verification, notably through simulations at a finer resolution, in more realistic wind conditions, or in a configuration with more than two turbines. This would help us to explain the differences observed between the two methods (disk-type and discrete-blade type) for the CW helix,both in terms of wake topology and power gains. Another open question following this paper concerns the phenomenology underlying the difference between CW and CCW helix. Understanding that may also contributed to explain why the two wind turbine representations produce different results for the CW helix.

Acknowledgments
This project has received funding from the European Research Council (ERC) under the European Union's Horizon2020 research and innovation program (grant agreement no. 725627). Computational resources were made available on the Tier-1 supercomputer of the Fédération Wallonie-Bruxelles, infrastructure funded by the Walloon Region (grant agreement no. 1117545), and on the supercomputers provided by the Consortium des Équipements de Calcul Intensif (CÉCI), funded by the Fonds de la Recherche Scientifique de Belgique (F.R.S.-FNRS) (grant agreement no. 2.5020.11).

References
[1] Meyers J, Bottasso C, Dykes K, Fleming P, Gebraad P, Giebel G, Göçmen T and van Wingerden J W 2022 Wind farm flow control: prospects and challenges *Wind Energy Science Discussions* **7** 2271–2306
[2] Frederik J, Doekemeijer B, Mulders S and van Wingerden J W 2020 The helix approach: Using dynamic individual pitch control to enhance wake mixing in wind farms *Wind Energy* **23** 1739–1751
[3] Moens M, Duponcheel M, Winckelmans G and Chatelain P 2018 An actuator disk method with tip-loss correction based on local effective upstream velocities *Wind Energy* **21** 766–782
[4] Chatelain P, Backaert S, Winckelmans G and Kern S 2013 *Proceedings of The 9th International Symposium on Engineering Turbulence Modelling and Measurements (ETMM-9), June 6–8, 2012, Thessaloniki, Greece* (*Flow, Turbulence and Combustion* vol 91) ed Rodi W ERCOFTAC (Springer) pp 587–605
[5] Caprace D G, Chatelain P and Winckelmans G 2019 Lifting line with various mollifications: theory and application to an elliptical wing *AIAA Journal* **57** 17–28
[6] Duponcheel M, Bricteux L, Manconi M, Winckelmans G and Bartosiewicz Y 2014 Assessment of RANS and improved near-wall modeling for forced convection at low Prandtl numbers based on LES up to $Re_\tau = 2000$ *International Journal of Heat and Mass Transfer* **75** 470–482 ISSN 0017-9310
[7] Winckelmans G S and Jeanmart H 2001 *Assessment of Some Models for LES without/with Explicit Filtering* (Dordrecht: Springer Netherlands) pp 55–66 ISBN 978-94-017-1263-7 URL `https://doi.org/10.1007/978-94-017-1263-7_7`
[8] Smagorinsky J General circulation experiments with the primitive equations *Monthly Weather Review* **91** 99–164
[9] Mann J 1998 Wind field simulation *Probabilistic Engineering Mechanics* **13** 269 – 282 ISSN 0266-8920
[10] Monaghan J 1985 Extrapolating B splines for interpolation *Journal of Computational Physics* **60** 253–262 ISSN 0021-9991
[11] Moens M, Coquelet M, Trigaux F and Chatelain P 2022 Handling individual pitch control within an actuator disk framework: verification against the actuator line method and application to wake interaction problems *Journal of Physics: Conference Series* **2265** 022053
[12] Chatelain P, Duponcheel M, Caprace D, Marichal Y and Winckelmans G 2017 Vortex particle-mesh simulations of vertical axis wind turbine flows: from the airfoil performance to the very far wake *Wind Energy Science* **2** 317–328 URL `https://www.wind-energ-sci.net/2/317/2017/`
[13] Caprace D G, Winckelmans G and Chatelain P 2020 An immersed lifting and dragging line model for the vortex particle-mesh method *Theoretical and Computational Fluid Dynamics* **34** 21–48
[14] Bossanyi E 2003 Individual blade pitch control for load reduction *Wind Energy* **6** 119–128
[15] Coleman R and Feingold A 1957 Theory of self-excited mechanical oscillations of helicopter rotors with hinged blades Tech. Rep. NACA-TN-3844
[16] Jonkman J, Butterfield S, Musial W and Scott G 2009 Definition of a 5-MW Reference Wind Turbine for Offshore System Development Tech. Rep. TP-500-38060 NREL